UCRL-JC-121628
PREPRINT
CONF-9510106--3

A Comparison of Nodular Defect Seed Geometeries from Different Deposition Techniques

C. Stolz, R. Tench,
M. Kozlowski, and A. Fornier

RECEIVED
FEB 06 1996
OSTI

This paper was prepared for submittal to the
Annual Symposium on Optical Materials
for High Power Lasers
Boulder, Colorado
October 30-November 1, 1995

December 29, 1995

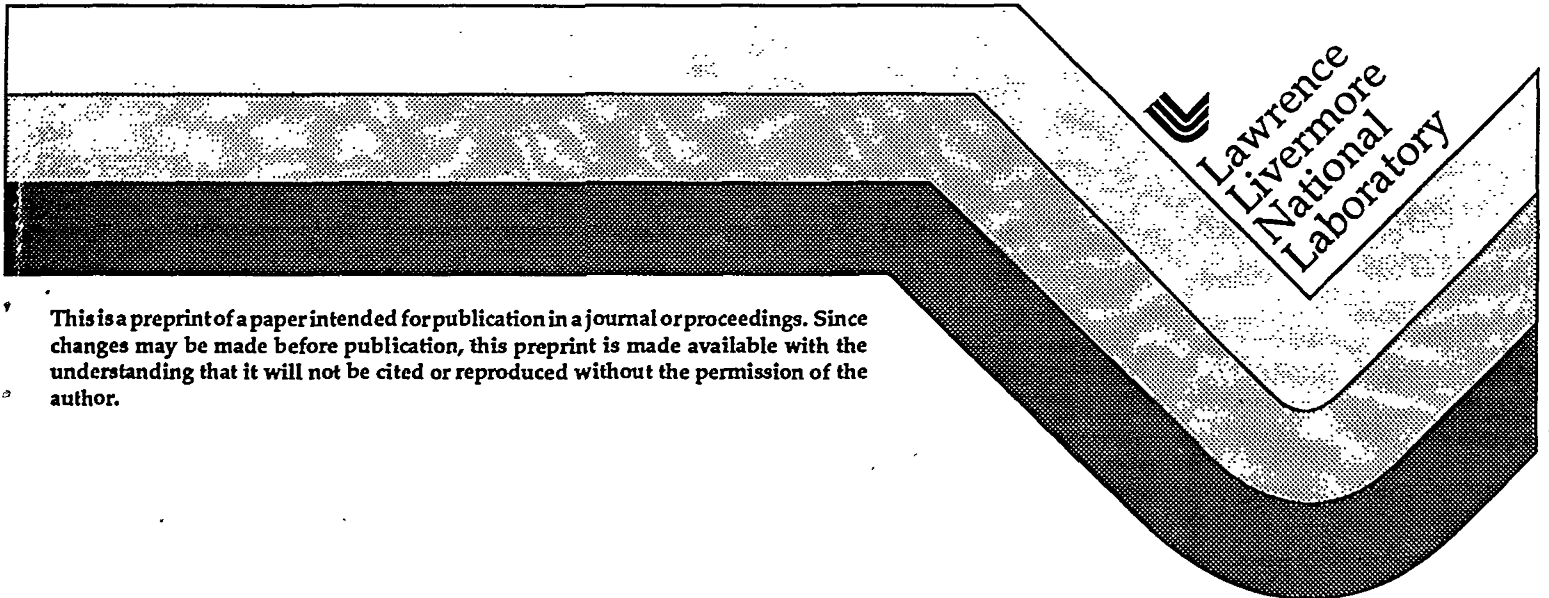

This is a preprint of a paper intended for publication in a journal or proceedings. Since changes may be made before publication, this preprint is made available with the understanding that it will not be cited or reproduced without the permission of the author.

MASTER

DISTRIBUTION OF THIS DOCUMENT IS UNLIMITED

DISCLAIMER

This document was prepared as an account of work sponsored by an agency of the United States Government. Neither the United States Government nor the University of California nor any of their employees, makes any warranty, express or implied, or assumes any legal liability or responsibility for the accuracy, completeness, or usefulness of any information, apparatus, product, or process disclosed, or represents that its use would not infringe privately owned rights. Reference herein to any specific commercial product, process, or service by trade name, trademark, manufacturer, or otherwise, does not necessarily constitute or imply its endorsement, recommendation, or favoring by the United States Government or the University of California. The views and opinions of authors expressed herein do not necessarily state or reflect those of the United States Government or the University of California, and shall not be used for advertising or product endorsement purposes.

A comparison of nodular defect seed geometeries from different deposition techniques

Christopher J. Stolz, Robert J. Tench, Mark R. Kozlowski, and Anne Fornier*

University of California
Lawrence Livermore National Laboratory
P. O. Box 808, L-487
Livermore, CA 94550

*C.E.A.-Centre d'Etudes de Limeil-Valenton
94195 Villeneuve Saint Georges Cedex
France

ABSTRACT

A focused ion-beam milling instrument, commonly utilized in the semiconductor industry for failure analysis and IC repair, is capable of cross-sectioning nodular defects. Utilizing the instrument's scanning on beam, high-resolution imaging of the seeds that initiate nodular defect growth is possible. In an attempt to understand the origins of these seeds, HfO_2/SiO_2 and Ta_2O_5/SiO_2 coatings were prepared by a variety of coating vendors and different deposition processes including e-beam, magnetron sputtering, and ion beam sputtering.

By studying the shape, depth, and composition of the seed, inferences of its origin can be drawn. The boundaries between the nodule and thin film provide insight into the mechanical stability of the nodule. Significant differences in the seed composition, geometry of nodular growth and mechanical stability of the defects for sputtered versus e-beam coatings are reported. Differences in seed shape were also observed from different coating vendors using e-beam deposition of HfO_2/SiO_2 coatings.

Key Words: Nodule, laser damage, focused ion-beam cross section, e-beam deposition, magnetron sputtering deposition, ion-beam sputtering deposition.

1. INTRODUCTION

Defects in multilayers have been studied for many years as initiation sites for laser damage.[1] These defects are created by particulates, either on the substrate surface before coating or deposited during the coating process. A nodule defect is created by overcoating the particulate or seed. Experimental data have been reported that illustrate a correlation exists between the susceptibility of laser damage, in the form of nodular ejection, and the diameter of the seed.[2,3] As the diameter of the seed decreases, the probability of ejection also decreases. To understand nodular ejection in optical coatings, a model of the thermally induced mechanical stresses has been proposed based on geometrical enhancements of the standing wave electric field (E-field).[4] The results of this model suggest the E-field is maximized by increasing the seed diameter or minimizing the depth of the seed in the multilayer. By studying these seeds in greater detail, coating manufacturers can infer their origins, allowing them to optimize their process to eliminate this source of laser damage to their optical coatings.

Two very promising techniques have been proposed for examining particulate generation during the coating process. Total internal reflection microscopy (TIRM) has been used for process optimization of magnetron sputtering to produce low defect density ZrO_2 films.[5] An in-situ particle monitor has also been developed and utilized for examining particulate generation during ion-beam sputtering (IBS) of Ta_2O_5 and SiO_2 multilayers.[6] Another way of examining defect seeds is by cross section. Previously it has been reported that a focused ion beam (FIB) can be used to cross-section nodules to expose defect seeds.[7,8] This technique, although limited to post deposition analysis, provides valuable insight into the seed composition, morphology, depth, and bonding to the host film. With this information, specific process improvements can be suggested, nodule stability can be better understood, and effects of different deposition processes on defect seed properties can be studied.

... page. Do not type or paste below this line.

... type anything on this line.

Write author's last name

2. EXPERIMENT

Optical coatings from multiple vendors were examined for analysis of defect seed morphology for slightly different e-beam deposition processes. Two material systems were examined, HfO_2/SiO_2 and Ta_2O_5/SiO_2 multilayers allowing the determination of starting material effects on seed composition. Finally, IBS and magnetron sputtering coatings were examined for comparison with e-beam films. The coatings were first examined under an optical microscope for identification of defects. Cross hairs were scratched on the surface near the defects to enable examination of a specific defect with multiple techniques. Care was taken to assure that fractures due to the cross hair generation did not affect the nodule. The defects were then measured on an atomic force microscope (AFM) to verify if the defect was a pit or nodule and to reveal any interesting surface features of the nodule. The samples were then overcoated with a few hundred angstroms of palladium to prevent surface charging, similar to standard scanning electron microscope (SEM) sample preparation techniques for non-conductive samples.

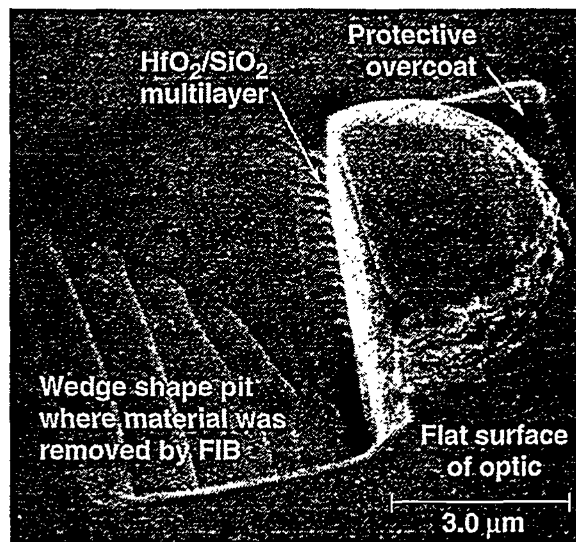

Figure 1. Overhead view of FIB cross-sectioned defect.

The samples were then placed in a FIB system for defect cross-sectioning. The FIB utilizes a liquid metal (usually gallium) ion source described elsewhere.[9,10] At high current, the beam is capable of milling the sample via sputtering. At low current, the FIB is a high resolution (~10 nm) scanning ion microscope (SIM), very similar to a SEM, and is utilized to identify the previously characterized defect and image the cross section. Once the defect is found, an area is selected for milling that includes one half of the defect. By inputting the physical thickness of the film, known from the coating design, and the width of the desired milled area, the computer calculates the required length of the triangular milling area to allow imaging of the cross section at a 60 degree angle as illustrated in figure 1. To prevent ejection of very weakly bound seeds during milling, a tungsten or metallic cap can be sputtered over the nodule. This additional layer also prevents rounding of the edge of the top coating layer, enabling better visualization of all edge boundaries. This instrument allows cross sectioning of well characterized nodules, precise positioning of the milled area (< 1 µm), and in-situ imaging of the cross section.

3. RESULTS

3.1 Seed diameter affects nodular stability

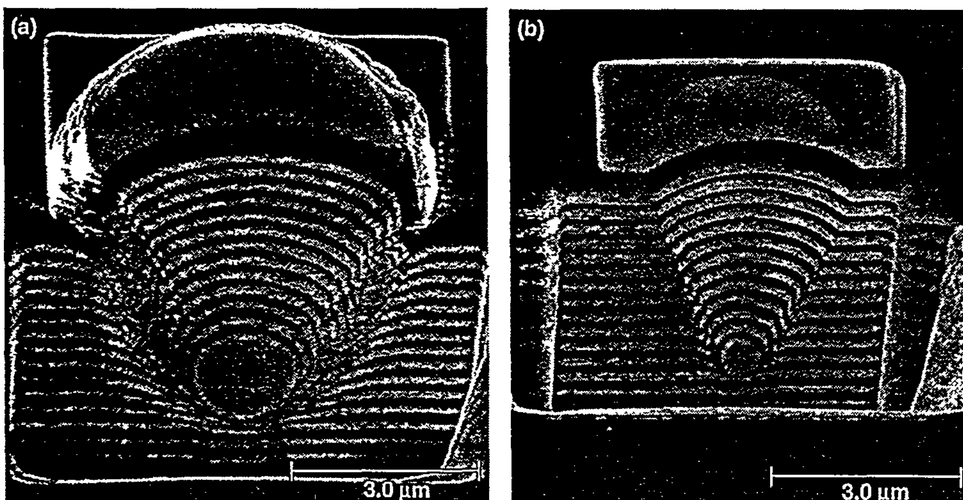

Figure 2. Seed diameter affects continuity of multilayer and nodule interface. (a) Large seed has very discontinuous boundry resulting in a mechanically unstable nodule. (b) Small seed has very continuous boundry resulting in a mechanically stable nodule.

The seed diameter has a significant impact on how well the nodule is attached to the coating. Large diameter seeds shadow the incoming coating flux causing voids as shown in figure 2a. These voids create discontinuous boundaries between the multilayer and nodule resulting in poor bonding. From a damage perspective, these poorly held defects cause benign damage when the nodule is ejected at a low fluence. This process, known as laser conditioning, creates high damage threshold pitson bygentle" nodule ejection.[11] If the seed is sufficiently deep, the outer coating layers of the multilayer and nodule will be become continuous, resulting in stronger bonding of the nodule. Although the mechanical stability of the nodule, and thereby the potential for its catastrophic failure increases as the seed depth increases, there is less E-field enhancement in these deep nodules and therefore a lower driving force for damage initiation. Small diameter seeds are well attached to the coating as shown in figure 2b and during laser irradiance have only moderate E-field enhancement and therefore have high damage thresholds. Medium diameter seeds appear to cause significant laser damage due to high E-field enhancements for shallower seeds and moderate bonding to the coating. Although the seed is weakly held due to the surrounding voids, the continuous outer coating layers attach the nodule to the coating leading to catastrophic damage in the top layers after nodule ejection.

3.2 Seed depth indicates time of seed deposition

A simple model has been proposed to describe the geometry of classic parabolic nodular defects.[12,13] The diameter of the nodule, D, is related to a constant, C, that is vendor specific, the seed diameter, d (which is also equal to the defect height, h), and depth, T, by the relation $D = (C \cdot d \cdot T)^{1/2}$. Previously reported cross sections of e-beam films have verified this parabolic behavior.[7,8] FIB cross sections that expose patterns in the seed depths suggest unique particulate generating events such as source "spitting" or arcing that can be correlated with process data taken during the coating run. Identification of events that result in defect seeds provide the coating manufacturer with the opportunity to address on those process parameters correlated to coating defect generation. Seeds randomly located throughout the multilayer indicate a more uniform generation of particulates. Since there is a direct relationship between defect depth and parameters that are measurable with an AFM, calculations of seed depths can be done in a nondestructive manner provided the constant, C, has been determined experimentally from measurements of FIB cross sections. It is worth noting that it is difficult to get a precise measurement of the defect depth of a cross section due to positioning errors of the FIB (~1 μm) that make it difficult to find the deepest part of the seed. If the seed is symmetrical and the cross section is not in the exact center, it should be possible to calculate the real depth of the seed based on AFM measurements of the nodule height. Unfortunately the majority of coating vendors have very complex seeds that lack the necessary amount of symmetry.

3.3 Seed morphology indicates phase of seed formation

In addition to affecting the height and width of the nodule, the seed also affects the surface profile of the nodule. Seeds with smooth boundaries result in nodules with classic dome shapes as shown in figure 3. Seeds with complex morphologies have very irregular surface features as shown in figure 4. Since the seed morphologies can be inferred from the surface features of the nodule, nondestructive AFM measurements can be used instead of destructive FIB measurements in some cases.

It has been previously suggested that different seed morphologies may be the result of the phase of the seed during it's formation.[7] If the seed resulted from a molten particulate ejected from the source material, one would expect the seed to have smooth edges and a very regular spherical or prolate-spheroid shape due to surface tension and gravitational forces. Seeds resulting from solid source ejection or arcing would have very irregular shapes and rough edges. For a given coating vendor, seeds are predominately smooth or rough indicating which processes should be optimized for elimination of a particulate source. One vendor is an exception with both smooth and rough edge seeds on the same coated sample as shown in figure 5. Given the size and shape of the seeds, they appear to be the result of both molten and solid particulate ejection from the source material.

Seeds have also been observed that do not appear to result from particulate ejection at the source. In figure 6 an elongated seed indicates a coating flake from the shutter mechanism as a probable seed source. Since this deposition process utilizes

Do not type anything on this line

HfO_2 (light layers), SiO_2 (dark layers) e-beam deposited from oxide starting materials

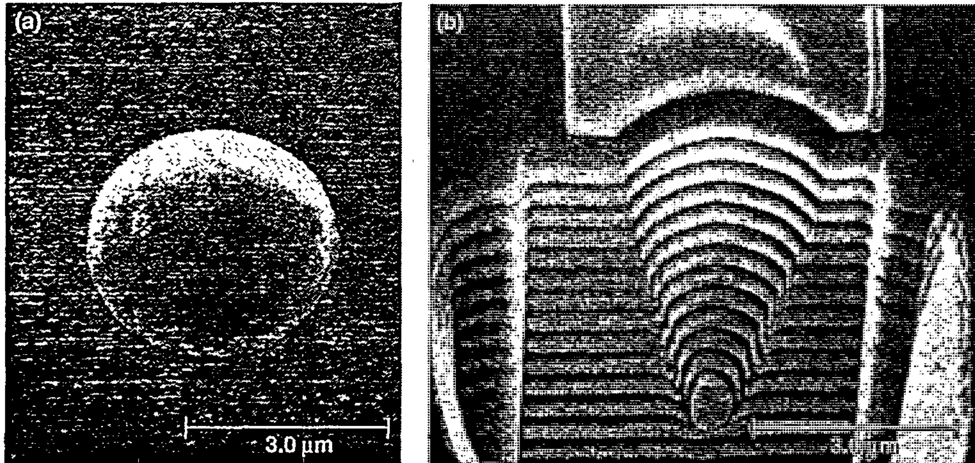

Figure 3. (a) Smooth dome topography of a "classic" nodule. (b) Cross section of nodule reveals smooth edged seed.

HfO_2 (light layers), SiO_2 (dark layers) e-beam deposited from oxide starting materials

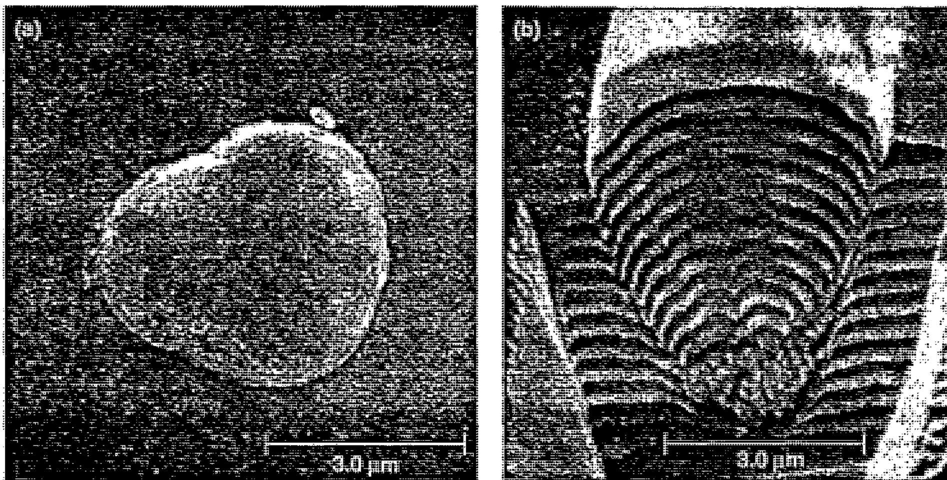

Figure 4. (a) Complex dome topography of a multilobe nodule. (b) Cross section of nodule reveals rough edged complex seed.

HfO_2 (light layers), SiO_2 (dark layers) e-beam deposited from oxide starting materials

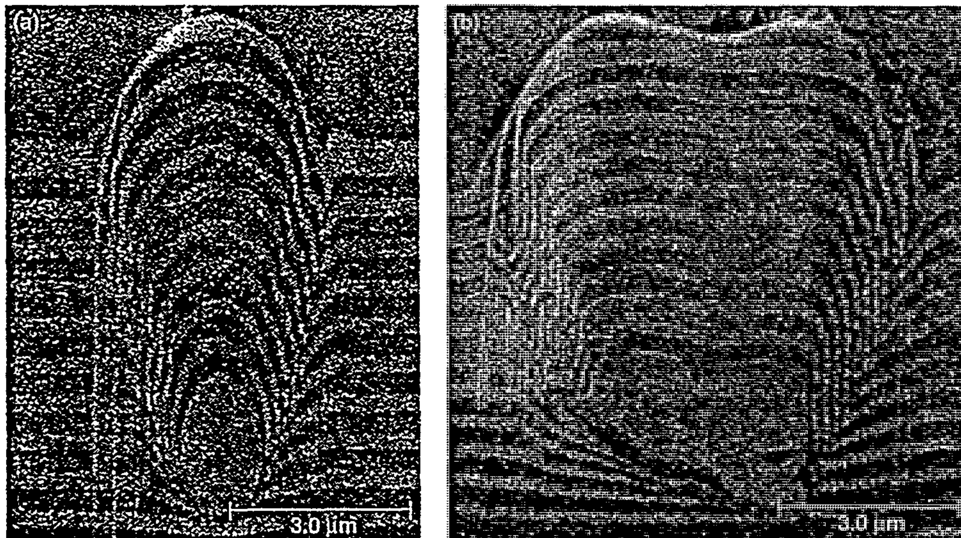

Figure 5. Cross sections from a coating reveal different seed morphologies. (a) Smooth edge seed indicates molten phase formation. (b) Rough edge seed indicates solid phase formation.

HfO_2 (light layers), SiO_2 (dark layers) e-beam deposited from Hf and SiO_2 starting materials

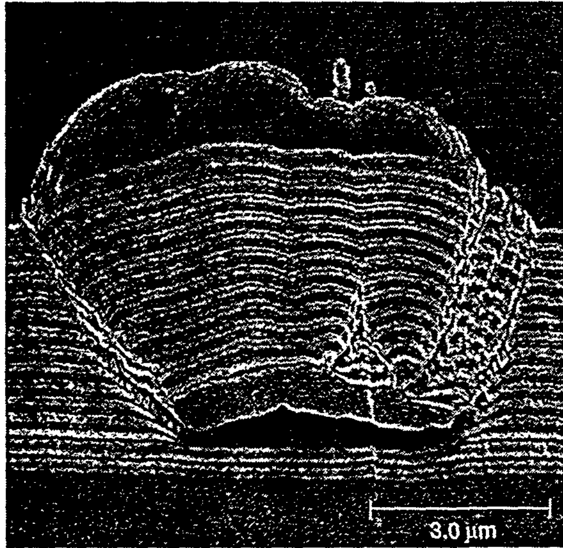

Figure 6. Elongated single material seed shape indicates cause of seed maybe a coating flake from the shutter mechanism.

HfO_2 (top three light layers), Ta_2O_5 (remaining light layers) SiO_2 (dark layers) IBS deposited from Hf, Ta, and SiO_2 targets

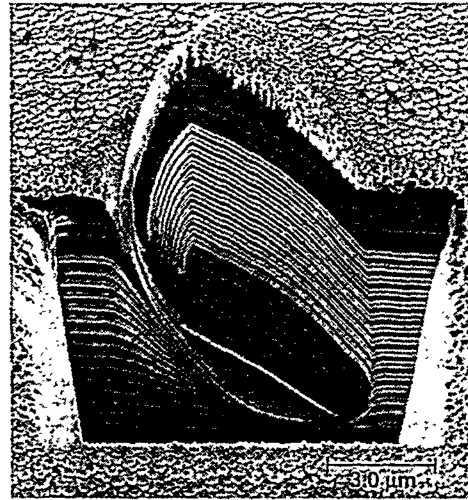

Figure 7. Seed consists of a multilayer that is three layers thick indicating seed source is a coating flake originating from a chamber surface.

different guns for different staring materials, the coating flakes from under the shutters consist of a single material. In figure 7, a coating flake that is three layers thick is the seed of the defect. The multilayer composition of the seed suggests a coating flake originating from one of the chamber surfaces.

3.4 Seed contrast indicates composition

By exploiting the different conductivities of the multilayer materials, one can infer the composition of the seed by comparison with the contrast of the individual multilayers. The light layers are the high-index material (HfO_2 or Ta_2O_5 in this study) and

HfO_2 (light layers), SiO_2 (dark layers) e-beam deposited from oxide starting materials

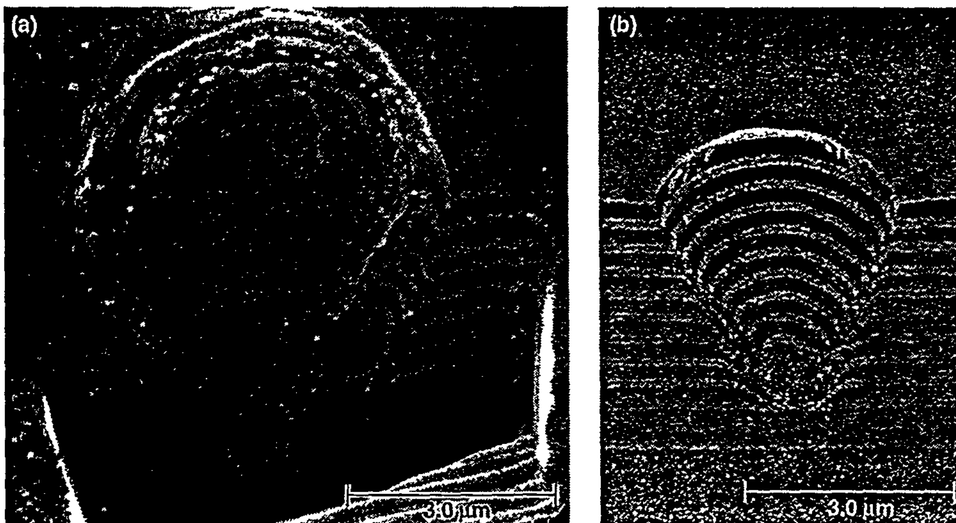

Figure 8. Seed contrast indicates seed composition. (a) Light seed indicates HfO_2 composition. (b) Dark seed indicates SiO_2 composition.

dark layers are SiO_2. Previously, Tench et. al., used scanning Auger microscopy to verify that the composition of light seeds from HfO_2/SiO_2 coatings was indeed an oxide of hafnium.[7] The vast majority of e-beam coatings deposited from oxide starting materials (HfO_2/SiO_2) that we examined had light seeds indicating HfO_2 composition as shown in figure 8a. One vendor is an exception where 40% of the cross sectioned seeds were dark, indicating SiO_2 composition as shown in figure 8b. It is worth noting that this vendor typically has lower defect density coatings (~20-40 defects/mm^2) than the other vendors (50-200 defects/mm^2) due to process optimization of the HfO_2 deposition. It is likely that SiO_2 seeds exist in e-beam coatings from other vendors, but in a significantly lower percentage so they have been elusive due to a limited number of defect cross sections.

Reactive evaporation of metallic hafnium has been suggested to reduce the defect densities in coatings.[14] We cross sectioned coatings all with very low defect densities (<10 defects/mm^2) deposited from metallic hafnium from three vendors. Only dark seeds, as shown in figure 9, have been found for two of the vendors and only light seeds as shown in figure 6 have been found for the third vendor. The light seeds, previously discussed, likely resulted from coating flakes from the underside of the shutter. It is also possible that particulates of oxidized Hf form at the edges of the molten pool. The dark seeds are most likely SiO_2, although scanning Auger microscopy should be performed for verification.

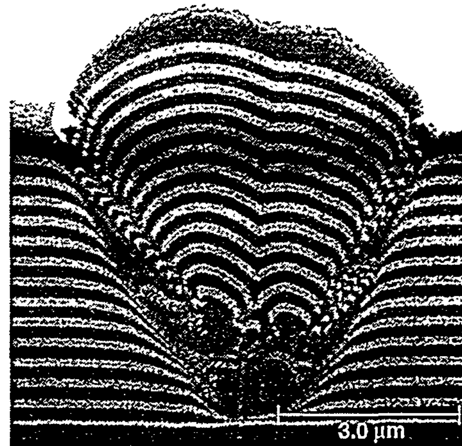

Figure 9. Typical defect seed from two vendors generated during deposition of metallic Hf and SiO_2. Defect densities were reduced significantly by modifying deposition process to evaporation of metallic instead of oxide form of Hf.

3.5 Seeds from other starting materials

Coatings from deposition of Ta_2O_5 and SiO_2 were also cross sectioned

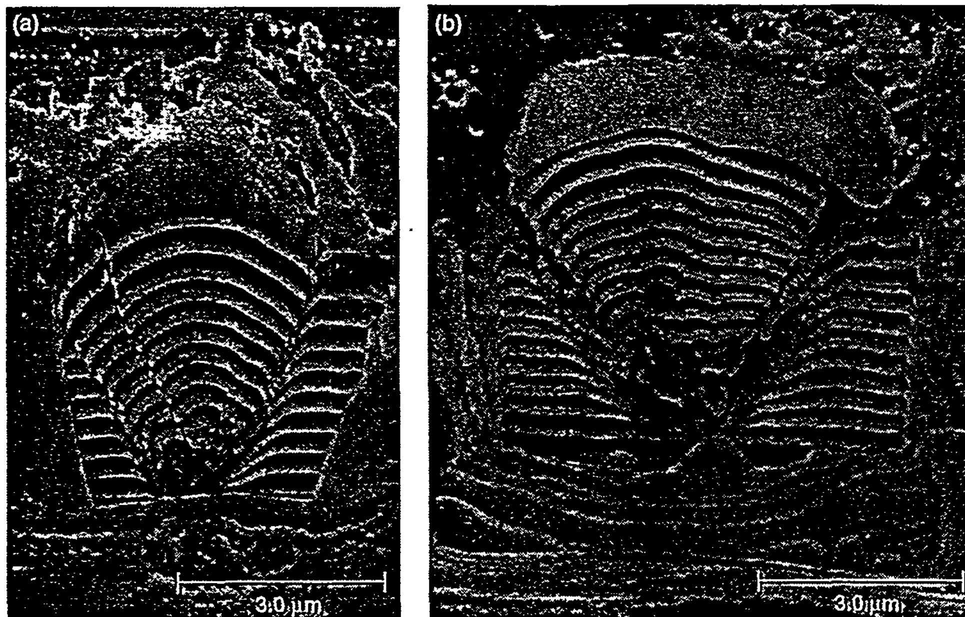

Figure 10. (a) Cross section containing seed. (b) Cross section where seed "fell out" before imaging.

Do not type anything on this line

as shown in figure 10a to understand the seed differences for different material combinations. This cross section illustrates some of the technical difficulties associated with this technique. For small seeds, it is difficult to position the FIB with enough accuracy to predictably cross section through the seed center. The further the cross section is from the center of the nodule, the less the confidence in the determination of the seed composition. One technique that we have utilized to increase our understanding of the three dimensional properties of the nodule is to take a series of cross sections starting near the nodule edge and continuing past the center. To illustrate this point, the defect in figure 11a has not been cross sectioned in the center of the nodule while the same defect has been cross sectioned in the center in figure 11b. These cross sections have illustrated how easy it is to misinterpret the seed composition if the cross section is through an adjacent layer and not the seed center.

An interesting feature of this particular nodule is the crack that propagates along the full length of the nodule. Since the

HfO_2 (light layers), SiO_2 (dark layers) e-beam deposited from Hf and SiO_2 starting materials

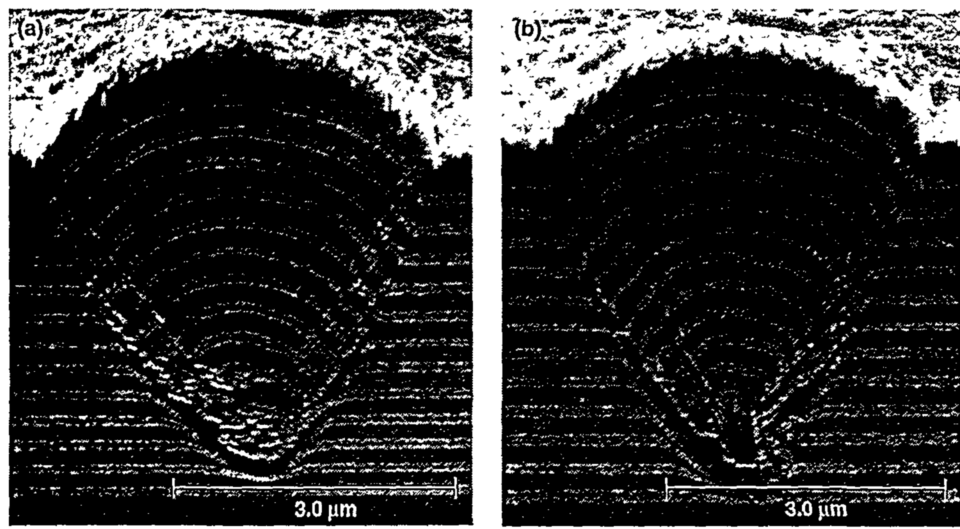

Figure 11. (a) Cross section not at center of nodule. (b) Cross section at nodule center reveals true seed composition.

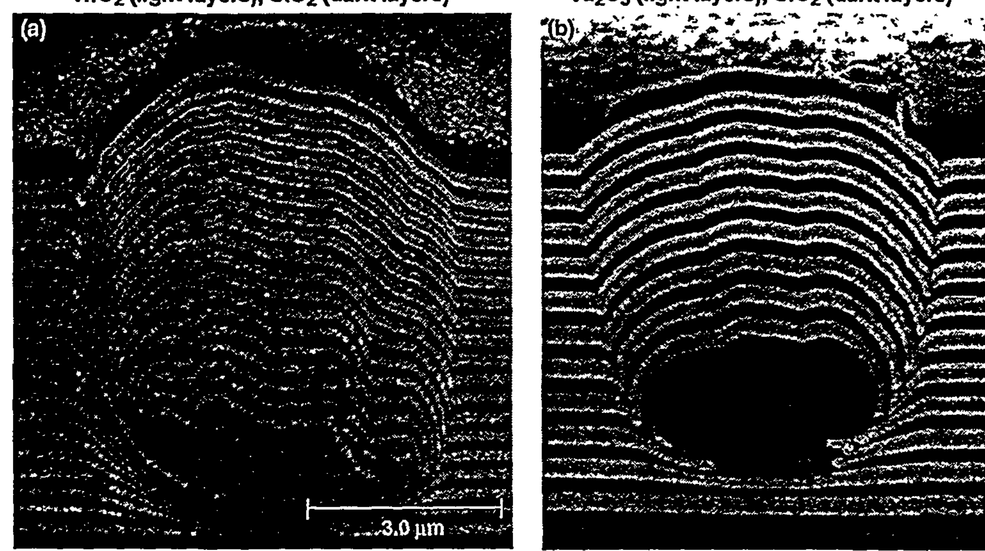

Figure 12. Cross section of typical defects from sputter deposition techniques. (a) IBS deposition of Hf and SiO_2. (b) Magnetron sputtering deposition of Ta and SiO_2.

Do not type anything on this line

multilayers do not align over any section of the crack, it must have formed after the deposition process. AFM evaluation of the surface of the nodule also revealed a surface discontinuity which indicated the crack was not the result of the cross-sectioning process. The existence of this crack suggests high mechanical stresses in the nodules, despite the presence of voids. Another problem that occurred when cross-sectioning this film was the instability of the seed as shown by the defect in figure 10b. During the cross-sectioning process, the seed was no longer bonded to the nodule and fell out before imaging. The same problem has been encountered on larger nodules, where the nodule was so unstable that it either fell apart during cross sectioning, or fell out before imaging.

3.6 Seeds of sputtered versus e-beam films

Two different sputtering process were evaluated-IBS and magnetron sputtering. The coatings were deposited from metallic high-index materials (Hf or Ta) and oxide low-index material (SiO_2). In both instances, despite the presence of large seeds, the interface between the coating and the nodule became continuous near the seed boundary as illustrated in figure 12. E-beam coatings with similar size nodules have very discontinuous, convoluted boundaries as illustrated in figure 2. This higher degree of mechanical stability with even large diameter seeds may result in significant collateral damage during nodule ejection and account for the lower damage thresholds observed in sputtered films.[14] Another interesting feature is the lack of parabolic shape to the nodule cross section over e-beam coatings. For both of these phenomena, the higher mobility of deposited material resulting from the more energetic sputtering process is the probable cause for the significant departure from e-beam nodule morphologies. The seeds for both sputtering processes are dark indicating SiO_2 composition. This is typical of most e-beam coatings deposited from Hf and SiO_2.

4. SUMMARY

Since defects are initiation sites for laser damage, FIB cross sections offer a unique tool to coating vendors for process optimization of low-defect-density film deposition processes. By studying the characteristics of the seeds, process modifications can be selected to solve a particular vendor's problems. Seed depth indicates time of seed deposition and may be correlated with unusual deposition events such as source "spitting" or arcing. Seed morphology indicates the phase of the seed during formation. Rough-edged seeds imply generation during a solid phase and smooth-edged seeds imply generation during a molten phase. Seed composition indicates which source material is creating the most significant number of seeds. Coating flakes from shutter mechanisms and other chamber surfaces can be identified by their shape and composition. Continuity of the boundary between the nodule and multilayer indicates mechanical stability of the nodule. This information can also be used for understanding the relationship of defect height and depth on laser damage susceptibility.

Process modifications such as changing the starting material from HfO_2 to Hf for e-beam deposition, yield lower defect densities and different chemistry seeds. These results imply that the high-index material is no longer the predominate source of particulate generation and that further refinement of the SiO_2 evaporation process is required for even lower defect density films.

5. ACKNOWLEDGMENTS

The following companies and individuals have contributed coatings and their expertise to make this paper possible: Dan Buntman at Accurel Systems, Marc von Gunten and Ron Bevis at Spectra-Physics, Ed Enemark and Tom Allen at Optical Coating Laboratory, Inc., Bernard Geenen at SFIM-ODS, Ramin Lalezari and Dale Long at Research Electro-Optics, Doug Smith at the Laboratory for Laser Energetics, Paul Szczepanski at Litton Airtron, and Norbert Kaiser and Axel Bodemann at Fraunhofer Instute in Jena, Germany. This work was performed under the auspices of the US Department of Energy by Lawrence Livermore National Laboratory under contract No. W-7405-Eng-48.

6. REFERENCES

1. D. Milam, and R. A. Bradbury, "The role of inclusions and linear absorption in laser damage to dielectric mirrors," in *Laser-Induced Damage in Optical Materials: 1973*, A. J. Glass, and A. H. Guenther, Eds., NBS Spec. Publ. 387, 124-132 (1973).

line of the page. Do not type or paste below this line

Do not type anything on this line.

Write author's last name

MS Page #

2. M. C. Staggs, M. R. Kozlowski, W. J. Siekhaus, and M. Balooch, "Correlation of damage threshold and surface geometry of nodular defects in HR coatings as determined by in-situ atomic force microscopy," in *Laser-Induced Damage in Optical Materials: 1992*, H. E. Bennett, A. H. Guenther, L. L. Chase, B. E. Newnam, and M. J. Soileau, eds., Proc. Soc. Photo-Opt Instrum. Eng. **1884**, 234-242 (1992).

3. M. R. Kozlowski, R. J. Tench, R. Chow, and L. Sheehan, "Influence of defect shape on laser-induced damage in multilayer coatings," in *Optical Interference Coatings*, F. Abelès, ed., Proc. Soc. Photo-Opt Instrum. Eng. **2253**, 743-750 (1994).

4. R. H. Sawicki, C. C Shang, and T. L. Swatlowski, "Failure characterization of nodular defects in multi-layer dielectric coatings," in *Laser-Induced Damage in Optical Materials: 1994*, H. E. Bennett, A. H. Guenther, M. R. Kozlowski, B. E. Newnam, and M. J. Soileau, eds., Proc. Soc. Photo-Opt Instrum. Eng. **2428**, 333-342 (1994).

5. F. L. Williams, G. A. Peterson, R. A. Schmell, and C. K. Carniglia, "Observation and control of thin-film defects using in-situ total internal reflection microscopy," in *Laser-Induced Damage in Optical Materials: 1991*, H. E. Bennett, A. H. Guenther, L. L. Chase, B. E. Newnam, and M. J. Soileau, eds., Proc. Soc. Photo-Opt Instrum. Eng. **1624**, 256-270 (1991).

6. R. G. Knollenberg, D. Long, and S. Lopez, "An in-situ fiber optics sensor for monitoring particle microcontamination during an IBS optical coating process," in *Optical Interference Coatings*, Vol. **17**, 1995 OSA Technical Digest Series (Optical Society of America, Washington DC), 124-126 (1995).

7. R. J. Tench, R. Chow, and M. R. Kozlowski, "Characterization of defect geometeries in multilayer optical coatings," in *Laser-Induced Damage in Optical Materials: 1993*, H. E. Bennett, A. H. Guenther, L. L. Chase, B. E. Newnam, and M. J. Soileau, eds., Proc. Soc. Photo-Opt Instrum. Eng. **2114**, 415-425 (1993).

8. R. J. Tench, M. R. Kozlowski, and R. Chow, "Investigation of the microstructure of coatings for high power lasers by non-optical techniques," in *Optical Interference Coatings*, Abelès, F., ed., Proc. Soc. Photo-Opt Instrum. Eng. **2253**, 596-2253 (1994).

9. P. Fischer, and J. Lindquist, "Failure analysis using focussed ion beams," Test & Measurement World, Nov. (1990).

10. J. M. Lindquist, R. J. Young, and M. C. Jaehnig, "Recent advances in application of focussed ion beam technology," Microelectronic Engineering, Vol. **21**, 179-186 (1993).

11. R. J. Tench, M. R. Kozlowski, J. Cohen, and R. Chow, "Laser damage and conditioning at defects in optical coatings," in *Optical Interference Coatings*, Vol. **17**, 1995 OSA Technical Digest Series (Optical Society of America, Washington DC), 214-216 (1995).

12. S. A. Letts, D. W. Myers, and L. A. Witt, "Ultrasmooth plasma polymerized coatings for laser fusion targets," J. Vac. Sci. Tech., Vol. **19**(3), 739-742, (1981).

13. R. J. Tench, R. Chow, and M. R. Kozlowski, "Characterization of defect geometeries in multilayer optical coatings," J. Vac. Sci. Tech., Vol. (1994).

13. R. Chow, S. Falabella, G. E. Loomis, F. Rainer, C. J. Stolz, and M. R. Kozlowski, "Reactive evaporation of low-defect density hafnia," Appl. Opt. Vol. **32**, 5567-5574 (1993).

14. C. J. Stolz, F. Y. Genin, M. R. Kozlowski, D. Long, R. Lalezari, Z. L. Wu, and P. K. Kuo, "Influence of microstructure on laser damage threshold of IBS coatings," in *Laser-Induced Damage in Optical Materials: 1995*, H. E. Bennett, A. H. Guenther, M. R. Kozlowski, B. E. Newnam, and M. J. Soileau, eds., Proc. Soc. Photo-Opt Instrum. Eng. **2714**, to be

Do not type anything on this line.

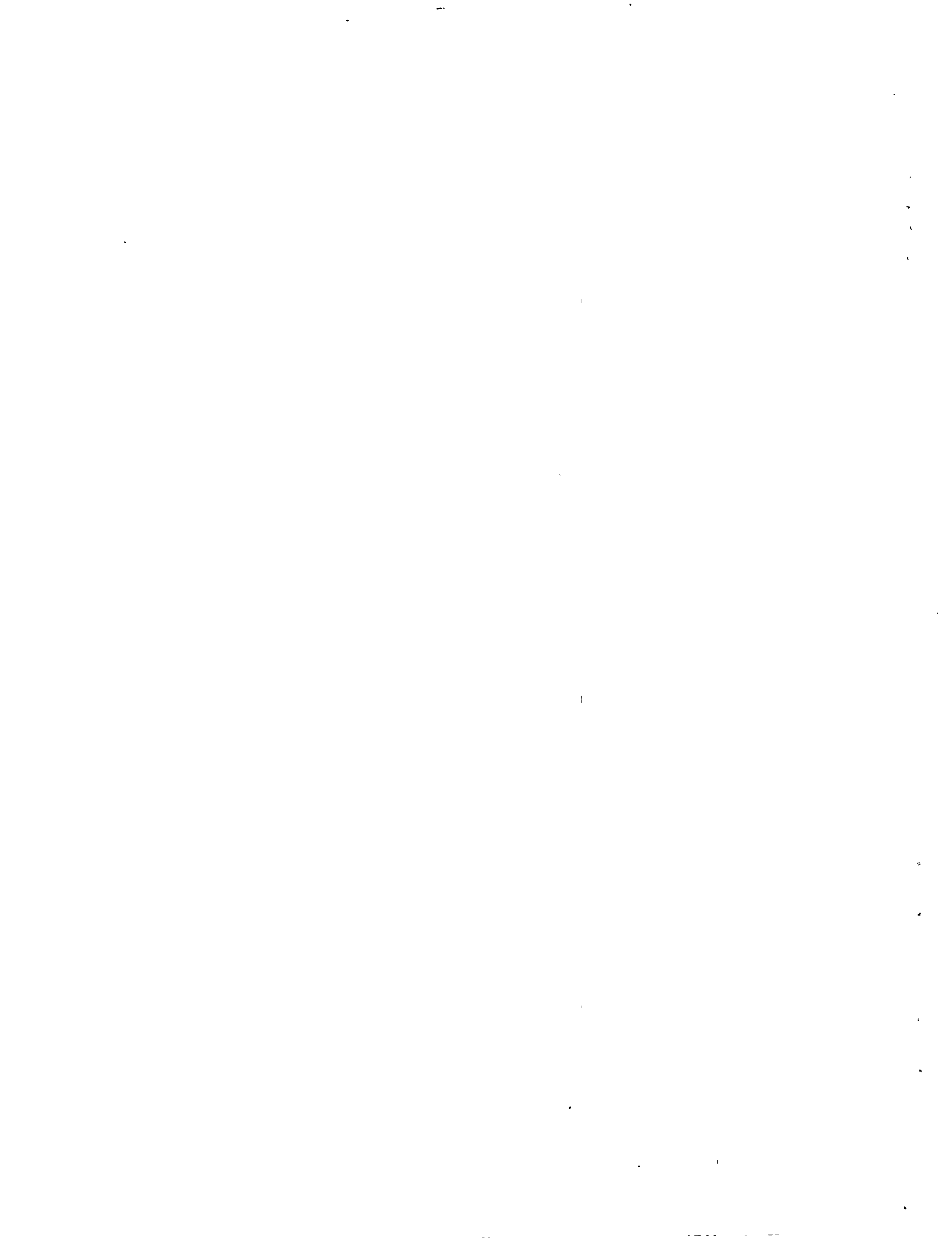

Technical Information Department • Lawrence Livermore National Laboratory
University of California • Livermore, California 94551